

Dipole-dipole scattering: summing large Pomeron loops in non-linear evolution with leading twist kernel

Eugene Levin^{1,*}

¹*Department of Particle Physics, Tel Aviv University, Tel Aviv 69978, Israel*

(Dated: February 4, 2026)

It is shown in this paper that the QCD equations for dipole density have the natural solution: the 'fan' diagrams of the Pomeron calculus. We found the dipole densities comparing the analytic solution to the Balitsky-Kovchegov (BK) equation for the simplified leading twist kernel with the t channel unitarity. Using these densities we calculate the contributions of large Pomeron loops to dipole-dipole scattering at high energies. Applying the Abramovsky,Gribov and Kancheli cutting rules we found that the produced gluons are distributed accordingly the KNO (Koba, Nielsen and Olesen) law which leads to the entropy $S_E = \ln(xG(x, Q^2))$ in an agreement with Kharzeev - Levin predictions.

PACS numbers: 13.60.Hb, 12.38.Cy

Contents

I. Introduction	1
II. Balitsky-Kovchegov non-linear equation for the leading twist BFKL kernel	3
III. Dipole densities and the BFKL Pomeron calculus	5
A. Pomeron solution to QCD evolution equations for ρ_n	5
B. Contributions of ρ_n to t -channel unitarity	7
IV. BK scattering amplitude in the BFKL Pomeron calculus	9
V. Multiplicity distribution and entropy of produced gluons for BK scattering amplitude	11
VI. Dipole-dipole scattering amplitude	14
VII. Multiplicity distribution of produced gluons for dipole-dipole scattering	15
VIII. Entropy of produced gluons	17
IX. Conclusions	17
References	18

I. INTRODUCTION

In this paper we continue [1–4] our attempts to sum large BFKL Pomeron loops[5]¹ for dipole-dipole scattering at high energies. The main goal of this paper is to expand our methods, suggested in our previous publications[2–4], to a wider range of energy going from ultra high energies to high energies in the saturation region. It is well known that the BFKL parton cascade leads to the non-linear Balitsky-Kovchegov (BK) equation [6, 7]. In Ref.[8] the analytical solution to this equation in the saturation region was found:

$$N^{\text{DIS}}(z = r^2 Q_s^2(Y, b)) = 1 - C(z) \exp\left(-\frac{z^2}{2\kappa}\right) \quad (1)$$

¹ BFKL stands for Balitsky, Fadin,Kuraev and Lipatov.

where $z = \ln(r^2 Q_s^2(Y))^2$. In our previous works we found that the sum of the large Pomeron loops leads to factor $\exp\left(-\frac{z^2}{4\kappa}\right)$ in the scattering amplitudes of dipole-dipoles, dipole-nucleus and nucleus-nucleus. In this paper we are going to discuss the smooth function $C(z)$ in Eq. (1) for dipole-dipole scattering. However at the moment we can do this for the simplified BFKL kernel: the BFKL kernel in the leading twist.

Summing Pomeron loops has been one of the difficult problems in the Color Glass Condensate (CGC) approach, without solving which we cannot consider the dilute-dilute and dense-dense parton densities collisions. However, in spite of intensive work [1–60], this problem has not been solved.

We sum the large Pomeron loops using the t -channel unitarity, which has been rewritten in the convenient form for the dipole approach to CGC in Refs.[9, 11, 12, 14, 15, 24, 25, 33, 34](see Fig. 1). The analytic expression takes the form [1, 12, 14]:

$$A(Y, r, R; \mathbf{b}) = \sum_{n=1}^{\infty} (-1)^{n+1} n! \int \prod_i^n d^2 r_i d^2 r'_i d^2 b'_i \int d^2 \delta b_i \gamma^{BA}(r_1, r'_i, \mathbf{b}_i - \mathbf{b}'_i \equiv \delta \mathbf{b}_i) \rho_n(Y - Y_0, \{r_i, \mathbf{b}_i\}) \rho_n(Y_0, \{r'_i, \mathbf{b}'_i\}) \quad (2)$$

γ^{BA} is the scattering amplitude of two dipoles in the Born approximation of perturbative QCD. The dipole densities $\rho_i(Y, \{r_i, \mathbf{b}_i\})$ have been introduced in Ref.[12] as follows:

$$\rho_n(r_1, b_1 \dots, r_n, b_n; Y - Y_0) = \frac{1}{n!} \prod_{i=1}^n \frac{\delta}{\delta u_i} Z(Y - Y_0; [u])|_{u=1} \quad (3)$$

where the generating functional Z is

$$Z(Y, \mathbf{r}, \mathbf{b}; [u_i]) = \sum_{n=1}^{\infty} \int P_n(Y, \mathbf{r}, \mathbf{b}; \{r_i, \mathbf{b}_i\}) \prod_{i=1}^n u(r_i, \mathbf{b}_i) d^2 r_i d^2 b_i \quad (4)$$

where $u(r_i, \mathbf{b}_i) \equiv u_i$ is an arbitrary function and P_n is the probability to have n dipoles with the given kinematics. The initial and boundary conditions for the BFKL cascade which stems from one dipole has the following form for the functional Z :

$$Z(Y = 0, \mathbf{r}, \mathbf{b}; [u_i]) = u(\mathbf{r}, \mathbf{b}); \quad Z(Y, r, [u_i = 1]) = 1; \quad (5a)$$

$$\rho_1(Y = 0, r, b, r_1, b_1) = \delta^{(2)}(\mathbf{r} - \mathbf{r}_1) \delta^{(2)}(\mathbf{b} - \mathbf{b}_1); \quad \rho_n(Y = 0, \mathbf{r}, \mathbf{b}; [r_i, b_i]) = 0 \text{ at } n \geq 2; \quad (5b)$$

In Eq. (2) $\mathbf{b}_i = \mathbf{b} - \mathbf{b}'_i$.

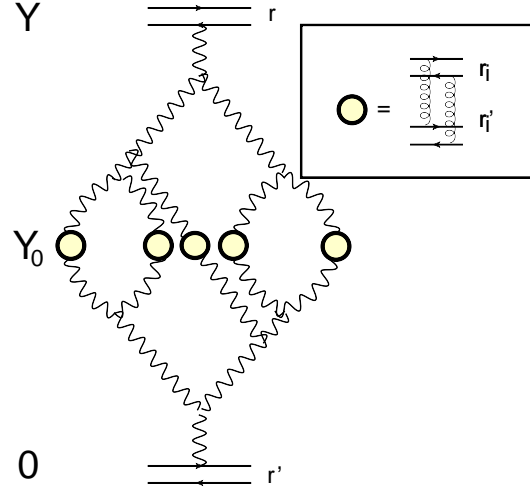


FIG. 1: Summing large Pomeron loops. The wavy lines denote the BFKL Pomeron exchanges. The circles denote the amplitude γ .

² We will discuss the definition of z and of κ in more detail below in Eq. (7) and in Eq. (9).

As one can see from Eq. (1) the BK equation leads to a new dimensional scale: saturation momentum[30] which has the following Y dependence[26, 30, 67]:

$$Q_s^2(Y, b) = Q_s^2(Y = 0, b) e^{\bar{\alpha}_S \kappa Y - \frac{3}{2\gamma_{cr}} \ln Y} \quad (6)$$

where $Y = 0$ is the initial value of rapidity and κ and γ_{cr} are determined by the following equations³:

$$\kappa \equiv \frac{\chi(\gamma_{cr})}{1 - \gamma_{cr}} = -\frac{d\chi(\gamma_{cr})}{d\gamma_{cr}} \quad (7)$$

where $\chi(\gamma)$ is given by

$$\omega(\bar{\alpha}_S, \gamma) = \bar{\alpha}_S \chi(\gamma) = \bar{\alpha}_S (2\psi(1) - \psi(\gamma) - \psi(1 - \gamma)) \quad (8)$$

The variable z that we have introduced in Eq. (1) has the following form:

$$z = \bar{\alpha}_S \frac{\chi(\bar{\gamma})}{\bar{\gamma}} (Y - Y_0) + \xi_{r,R} \quad (9)$$

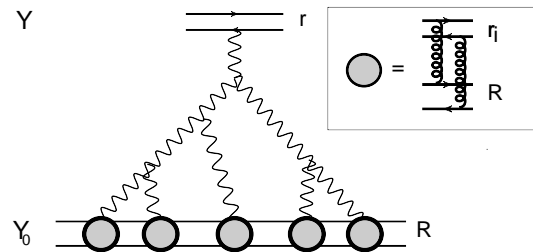


FIG. 2: The non-linear BK equation. The wavy lines denote the BFKL Pomeron exchanges. The circles denote the amplitude γ for interaction of the dipole with the target.

In the next section we review the Balitsky-Kovchegov (BK) non-linear equation for the simplified, leading twist BFKL kernel. We will discuss the solution to this equation which has a simple analytic form for this kernel. In section III we show how this solution can be reconciled with the BFKL Pomeron calculus. We demonstrate that the natural solution to the QCD evolution equations for dipole densities ρ_n is the 'fan' BFKL Pomeron diagrams. In this section we also discuss how ρ_n contribute to summing large Pomeron loops.

In section IV we find the BK scattering amplitude as a sum of many Pomerons exchanges and in doing so we reconstruct the densities ρ_n . We also discuss and find the way to sum the asymptotic series of the multi Pomeron exchanges that lead to the scattering amplitude. In section V we use the advantage of the multi Pomeron series for the scattering amplitude and calculated the multiplicity distributions based on s-channel unitarity for the BFKL Pomeron and the AGK cutting rules.

In section VI we calculate the scattering amplitude for the dipole-dipole scattering using Eq. (2) and in section VII we present our calculations of the multiplicity distribution for the dipole-dipole amplitude. In section VIII we show that the entropy of the produced gluons for both processes give $S_E = \ln(xG(x, Q^2))$ where xG is the gluon structure function. Therefore it confirms the result of Ref.[70]. In conclusion we summarize our results and discuss possible flaw in our approach,

II. BALITSKY-KOVCHEGOV NON-LINEAR EQUATION FOR THE LEADING TWIST BFKL KERNEL

The scattering matrix (S-matrix) of the colourless dipole with the size x_{01} satisfies the Balitsky-Kovchegov (BK) non-linear equation[6, 7]:

$$\frac{\partial S_{01}}{\partial Y} = \bar{\alpha}_S \int \frac{d^2 x_{02}}{2\pi} \frac{x_{01}^2}{x_{02}^2 x_{12}^2} \left\{ S_{02} S_{12} - S_{01} \right\} \quad (10)$$

³ $\chi(\gamma)$ is the BFKL kernel[5] in anomalous dimension (γ) representation. ψ is the Euler psi -function (see Ref.[69] formula 8.36).

where $S_{ik} = S(Y, \mathbf{x}_{ik}, \mathbf{b})$ ⁴ is the scattering matrix of the dipoles with size x_{ik} and with rapidity Y at the impact parameter \mathbf{b} . For the full BFKL kernel the solution at ultra high energy comes from Eq. (10) assuming that $S_{02}(S_{12})$ are small, Eq. (10) degenerates to

$$\frac{\partial S_{01}}{\partial Y} = -\bar{\alpha}_S \int \frac{d^2 x_{02}}{2\pi} \frac{x_{01}^2}{x_{02}^2 x_{12}^2} S_{01} \quad (11)$$

For the geometric scaling solution inside the saturation region[62] Eq. (11) can be rewritten as follows[8]:

$$\kappa \frac{dS_{01}(z)}{dz} = -z S_{01}(z) \quad (12)$$

with the solution:

$$S_{01}(z) = C(z) \exp\left(-\frac{z^2}{2\kappa}\right) \quad (13)$$

where $C(z)$ is a smooth function. In this derivation we consider that the reggeization of gluon gives $\bar{\alpha}_S \ln(x_{01}^2 Q_s^2(Y)) = \bar{\alpha}_S z$. Unfortunately we are not ready at the moment to provide solution for $C(z)$ in Eq. (13) for the general BFKL kernel. We will specify the solution in the entire region of z in the saturation region for the simplified BFKL kernel suggested in Ref.[8]. This kernel describes the high energy asymptotic solution of the nonlinear BK equation and leads to the geometric scaling behaviour.:

$$\chi(\gamma) = \begin{cases} \frac{1}{1-\gamma} & \text{for } z = \xi_{r,R} + \kappa \bar{\alpha}_S Y > 0, \text{ summing } (z)^n; \\ \frac{1}{\gamma} & \text{for } z < 0, \text{ summing } (\xi)^n; \end{cases} \quad (14)$$

where $\kappa = 4$ for this kernel and $\xi_{r,R}$ will be defined in Eq. (21) below.

Since this kernel sums log contributions it corresponds to leading twist term of the full BFKL kernel. It has a very simple form in the coordinate representation [8]:

$$\int K(\mathbf{r}', \mathbf{r} - \mathbf{r}' | \mathbf{r}) d^2 r' \rightarrow \frac{\bar{\alpha}_S}{2} \int_{1/Q_s^2(Y,b)}^{r^2} \frac{dr'^2}{r'^2} + \frac{\bar{\alpha}_S}{2} \int_{1/Q_s^2(Y,b)}^{r^2} \frac{d|\mathbf{r} - \mathbf{r}'|}{|\mathbf{r} - \mathbf{r}'|^2} = \frac{\bar{\alpha}_S}{2} \int_{\xi_s}^{\xi} d\xi_{r'} + \frac{\bar{\alpha}_S}{2} \int_{\xi_s}^{\xi} d\xi_{\mathbf{r}-\mathbf{r}'} \quad (15)$$

where $\xi_{r'} = \ln\left(\frac{r'^2 r_1^2}{b^4}\right)$ for $b > r, r_1$ and $\xi_s = \kappa \bar{\alpha}_S Y$ for the scattering of the dipole r' with the dipole r_1 . Note, that the logarithms originate from the decay of a large size dipole, into one small size dipole and one large size dipole[8]. However, the size of the small dipole is still larger than $1/Q_s^2 = \frac{b^4}{r_1^2} e^{-\kappa Y}$. Using Eq. (15) and Eq. (10) we can obtain the non-linear equation for the scattering amplitude $N_{i,k} = 1 - S_{ik} = 1 - S(Y, \mathbf{x}_{ik}, \mathbf{b})$ in the simple form:

$$\frac{\partial N(Y, \xi, b)}{\partial Y} = \bar{\alpha}_S (1 - N(Y, \xi', b)) \int_{\xi_s}^{\xi} d\xi' N(Y, \xi', b) \quad (16)$$

and for the geometric scaling solution:

$$4 \frac{dN(z)}{dz} = (1 - N(z)) \int_0^z dz' N(z') \quad (17)$$

The general solution for the linear equation has the following form:

$$N_{\text{lin}}(z) = C_1 e^{\frac{1}{2}z} + C_2 e^{-\frac{1}{2}z} \quad (18)$$

⁴ For simplicity we assume that $b \gg r_{i,k}$. The equation without this assumption has a bit more cumbersome form and can be found in Ref.[9], for example.

The second solution decreases at large z and could be important only at the border of the saturation region. The first solution is the BFKL Pomeron exchange which satisfy the boundary condition at $z = 0$ [26, 30], viz.

$$G_{IP}(z) = N_0 e^{\bar{\gamma} z} \quad (19)$$

where $\bar{\gamma} = 1 - \gamma_{cr} = \frac{1}{2}$, N_0 is a constant. $G_{IP}(z)$ is the Green's function of the BFKL Pomeron exchange. For exchanges of n BFKL Pomerons we have the Green's function in the form:

$$G_{nIP} = (G_{IP}(z))^n \quad (20)$$

z in Eq. (18) and Eq. (20) is defined by Eq. (9) (see Fig. 2) where $\xi_{r,R}$ we can find from the eigenfunction of the BFKL equation with the eigenvalue $\bar{\alpha}_S \chi(\gamma)$ (the scattering amplitude of two dipoles with sizes r and R) which has the following form [13]

$$\phi_\gamma(\mathbf{r}, \mathbf{R}, \mathbf{b}) = \left(\frac{r^2 R^2}{(\mathbf{b} + \frac{1}{2}(\mathbf{r} - \mathbf{R}))^2 (\mathbf{b} - \frac{1}{2}(\mathbf{r} - \mathbf{R}))^2} \right)^\gamma = e^{\gamma \xi_{r,R}} \text{ with } 0 < \text{Re } \gamma < 1 \quad (21)$$

Eq. (16) can be rewritten in a simpler form for $\Omega(\xi_s, \xi)$: $N(Y, \xi, b) = 1 - \exp(-\Omega(\xi_s, \xi))$, with $\xi_s = \bar{\alpha}_S \kappa Y$. It takes the form:

$$\frac{\partial^2 \Omega(\xi_s, \xi)}{\partial \xi_s \partial \xi} = \frac{1}{4} (1 - e^{-\Omega(\xi_s, \xi)}) \quad (22)$$

Eq. (22) has the geometric scaling solution (see formula **3.5.3** in Ref.[65]), which has the following implicit form:

$$\sqrt{2} \int_{\Omega_0}^{\Omega(z)} \frac{d\Omega'}{\sqrt{\Omega' - 1 + \exp(-\Omega')}} = z \quad (23)$$

In Eq. (23) Ω_0 is the initial condition for $\Omega(z)$: $\Omega(z=0) = \Omega_0$. Note, that N_0 in Eq. (19) is equal to $N_0 = 1 - \exp(\Omega_0) \xrightarrow{\Omega_0 \ll 1} \Omega_0$. Eq. (23) has two analytical solution for small and large z . Indeed, for $z \ll 1$ $\Omega(z)$ in Eq. (23) is close to Ω_0 and for small Ω_0 Eq. (23) can be written as follows:

$$2 \int_{\Omega_0}^{\Omega(z)} \frac{d\Omega'}{\Omega'} = z \quad (24)$$

leading to $\Omega(z) = \Omega_0 e^{\frac{1}{2}z}$. Hence, the solution of Eq. (23) satisfies the initial conditions of Eq. (19).

For $z \gg 1$ we can consider Ω' to be large and approximate Eq. (23) by

$$\sqrt{2} \int_{\Omega_0}^{\Omega(z)} \frac{d\Omega'}{\sqrt{\Omega'}} = z \quad (25)$$

which gives $\Omega(z) = \frac{1}{8}z^2$ in accord with Eq. (13).

Fig. 3 shows how these analytical limits describe the exact $\Omega(z)$. One can see that correction to the asymptotic behaviour at large z is rather large leading to $\frac{1}{8}z^2 - \Omega_{exact}(z) \approx z$.

The main goal of this paper to obtain information on the dipole densities (ρ_n of Eq. (2)) from Eq. (18).

III. DIPOLE DENSITIES AND THE BFKL POMERON CALCULUS

A. Pomeron solution to QCD evolution equations for ρ_n

The evolution equations for ρ_n have been derived in QCD for the BFKL cascade in Ref.[12], and for $\bar{\rho}_n(\mathbf{r}, \mathbf{b}; \{r_i, b_i\})$ defined as

$$\bar{\rho}_n(\mathbf{r}, \mathbf{b}; \{r_i, b_i\}) = \prod_{i=1}^n r_i^2 \rho_n(\{r_i, b_i\}) \quad (26)$$

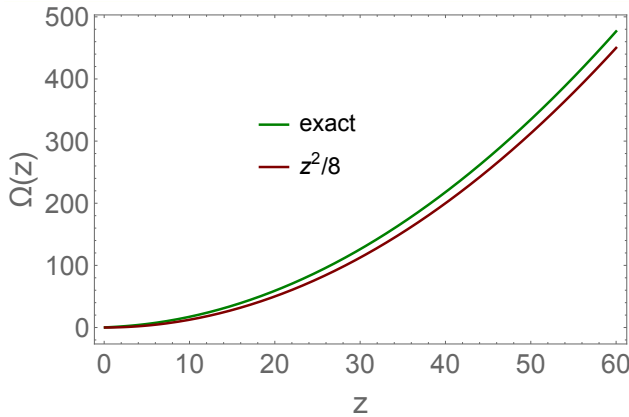


Fig. 3-a

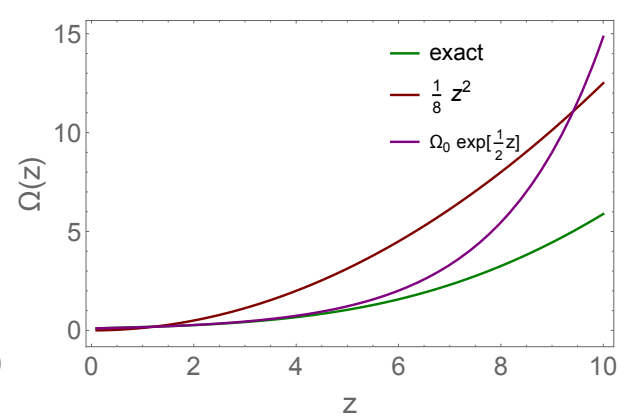


Fig. 3-b

FIG. 3: $\Omega(z)$ versus z . Ω_{exact} is the numerical solution of Eq. (23) with $\Omega_0 = 0.1$. Fig. 3-a shows the large range of z , while Fig. 3-b is concentrated at small $z < 10$ to illustrate how the exchange of the BFKL Pomeron describes $\Omega(z)$.

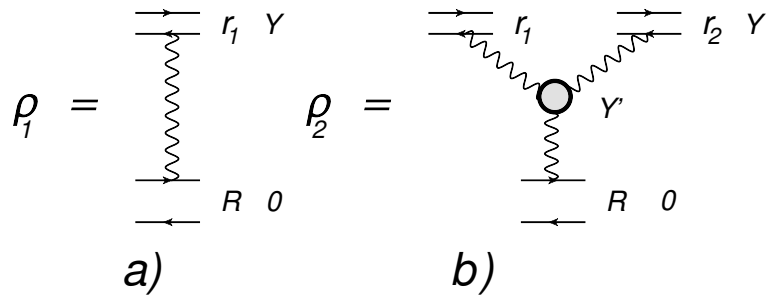


FIG. 4: The dipole densities in the BFKL Pomeron calculus. Fig. 4-a shows that ρ_1 is given by the exchange of the BFKL Pomeron. Fig. 4-b demonstrates that ρ_2 is the contribution of the first 'fan' diagram of the BFKL Pomeron calculus. The wavy lines denote the BFKL Pomeron exchanges. The circle denotes the triple Pomeron vertex, given by the BFKL kernel.

they have the following form

$$\begin{aligned} \frac{\partial \bar{\rho}_n(\{\mathbf{r}_i, \mathbf{b}_i\})}{\partial Y} &= \sum_{i=1}^n \int \frac{d^2 r'}{2\pi} K(\mathbf{r}', \mathbf{r}_i - \mathbf{r}' | \mathbf{r}_i) \\ &\times \left\{ \bar{\rho}_n(\{\mathbf{r}_j, \mathbf{b}_j\}, \mathbf{r}', \mathbf{b}_i - (\mathbf{r}_i - \mathbf{r}')/2) + \bar{\rho}_n(\{\mathbf{r}_j, \mathbf{b}_j\}, \mathbf{r}_i - \mathbf{r}', \mathbf{b}_i - \mathbf{r}'/2) - \bar{\rho}_n(\{\mathbf{r}_i, \mathbf{b}_i\}) \right\} \\ &+ \bar{\alpha}_S \sum_{i=1}^{n-1} \bar{\rho}_{n-1}(\dots, \mathbf{r}_i + \mathbf{r}_n, b_{in} \dots). \end{aligned} \quad (27)$$

This set of equations has been derived without assuming that the BFKL Pomeron calculus is the realization of the Color Glass Condensate (CGC) approach. In this section it will be shown that Eq. (27) has a natural solution in the BFKL Pomeron calculus reproducing the sum of the 'fan' diagrams.

Let us start with $\bar{\rho}_1$, for which we have the following equation:

$$\frac{\partial \bar{\rho}_1(Y; \mathbf{r}_1, \mathbf{b}_1)}{\partial Y} = \int \frac{d^2 r'}{2\pi} K(\mathbf{r}', \mathbf{r}_1 - \mathbf{r}' | \mathbf{r}_1) \left\{ \bar{\rho}_1(Y; \mathbf{r}', \mathbf{b}_1 - (\mathbf{r}_1 - \mathbf{r}')/2) + \bar{\rho}_1(Y; \mathbf{r}_1 - \mathbf{r}', \mathbf{b}_1 - \mathbf{r}'/2) - \bar{\rho}_1(Y; \mathbf{r}_1, \mathbf{b}_1) \right\} \quad (28)$$

Hence one can see that ρ_1 is the solution to the BFKL equation and, therefore, describes the BFKL Pomeron exchange (see Fig. 4-a). Using Eq. (15) for the leading twist BFKL kernel and considering b being larger than r_1 and r' one can see that Eq. (28) is given by Eq. (19).

Our the next step is to show that the first fan diagram of Fig. 4-b gives the solution of Eq. (27) for $\bar{\rho}_2$. The

contribution of this diagram has the following form (see Fig. 4-b):

$$\bar{\rho}_2(Y; \mathbf{r}_1, \mathbf{b}_1, \mathbf{r}_2, \mathbf{b}_2) = \int_0^Y dY' \int G_{\mathcal{P}}(Y - Y', \xi_{r_1, r'_1}) G_{\mathcal{P}}(Y - Y', \xi_{r_2, r'_2}) d^2 r'_1 \underbrace{K(r'_1, r'_2 | r'_1 + r'_2)}_{\text{triple Pomeron vertex}} \frac{d^2(r'_1 + r'_2)}{(r'_1 + r'_2)^2} G_{\mathcal{P}}(Y', \xi_{r'_1 + r'_2, R}) \quad (29)$$

Taking derivative with respect to Y we get:

$$\begin{aligned} \frac{\partial \bar{\rho}_2(Y; \mathbf{r}_1, \mathbf{b}_1, \mathbf{r}_2, \mathbf{b}_2)}{\partial Y} = & \int_0^Y dY' \int \frac{\partial G_{\mathcal{P}}(Y - Y', \xi_{r_1, r'_1})}{\partial Y} G_{\mathcal{P}}(Y - Y', \xi_{r_2, r'_2}) d^2 r'_1 K(r'_1, r'_2 | r'_1 + r'_2) \frac{d^2(r'_1 + r'_2)}{(r'_1 + r'_2)^2} G_{\mathcal{P}}(Y', \xi_{r'_1 + r'_2, R}) \\ & + \int_0^Y dY' \int G_{\mathcal{P}}(Y - Y', \xi_{r_1, r'_1}) \frac{\partial G_{\mathcal{P}}(Y - Y', \xi_{r_2, r'_2})}{\partial Y} d^2 r'_1 K(r'_1, r'_2 | r'_1 + r'_2) \frac{d^2(r'_1 + r'_2)}{(r'_1 + r'_2)^2} G_{\mathcal{P}}(Y', \xi_{r'_1 + r'_2, R}) \\ & + \int G_{\mathcal{P}}(0, \xi_{r_1, r'_1}) G_{\mathcal{P}}(0, \xi_{r_2, r'_2}) d^2 r'_1 K(r'_1, r'_2 | r'_1 + r'_2) \frac{d^2(r'_1 + r'_2)}{(r'_1 + r'_2)^2} G_{\mathcal{P}}(Y, \xi_{r'_1 + r'_2, R}) \end{aligned} \quad (30)$$

The first two terms of this equations reproduce the first two terms of Eq. (27) for ρ_2 since $G_{\mathcal{P}}(Y - Y', \xi_1 - \xi'_1)$ as well as $G_{\mathcal{P}}(Y - Y', \xi_2 - \xi'_2)$ satisfy the BFKL equations.

Using the initial conditions of Eq. (5b) for $\rho_1(Y = 0, r_1, b_1) = G_{\mathcal{P}}(0, \xi_1 - \xi'_1)$ ($\rho_1(Y = 0, r_2, b_2) = G_{\mathcal{P}}(0, \xi_2 - \xi'_2)$) one can see that the last term in Eq. (30) is equal to $\rho_1(Y, \mathbf{r}_1 + \mathbf{r}_2, \mathbf{b})$. Therefore, Eq. (29) gives the solution to Eq. (27) for ρ_2 .

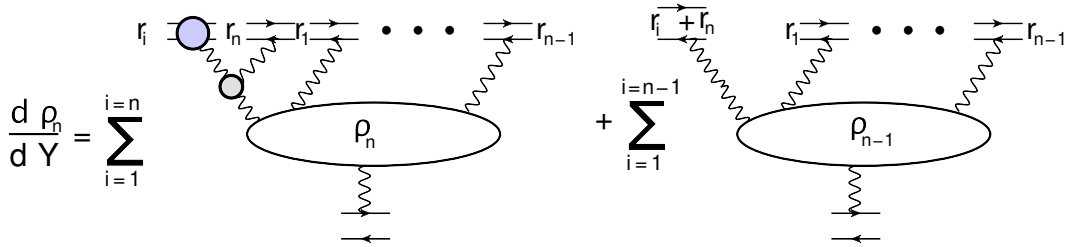


FIG. 5: The graphic form of the equation for ρ_n in the BFKL Pomeron calculus. in the BFKL Pomeron calculus. The wavy lines denote the BFKL Pomeron exchanges. The black circle denotes the triple Pomeron vertex, given by the BFKL kernel. The blue circles stand for the BFKL kernels

Actually, this proof shows a general pattern: the derivatives with respect of Y of $G_{\mathcal{P}}^n$ lead to the first term in Eq. (27) for ρ_2 , while $Y' = Y$ gives the second term in Eq. (27) due to the initial conditions. The graphic form of this general derivation one can see in Fig. 5.

B. Contributions of ρ_n to t-channel unitarity

In this section we wish to show, that actually only the first term in the evolution equations for ρ_n (see Eq. (27)), contribute to the t -channel unitarity of Eq. (2). This term gives the large Pomeron loop diagrams, while the second term leads to the corrections which we cannot control.

Let us calculate Eq. (29) for the leading twist BFKL kernel using Eq. (19) for $G_{\mathcal{P}}$ and Eq. (15) for the kernel. In addition we take into account the initial condition of Eq. (5b). Integration over Y' results in the following expression:

$$\begin{aligned}
\bar{\rho}_2(Y; \mathbf{r}_1, \mathbf{b}_1, \mathbf{r}_2, \mathbf{b}_2) = & \\
& \frac{1}{2} \int G_{\mathbb{P}}(Y - Y', \xi_{r_1, r'_1}) G_{\mathbb{P}}(Y - Y', \xi_{r_2, r'_2}) d^2 r'_1 K(\mathbf{r}'_1, \mathbf{r}'_2 | \mathbf{r}'_1 + \mathbf{r}'_2) \frac{d^2(\mathbf{r}'_1 + \mathbf{r}'_2)}{(\mathbf{r}'_1 + \mathbf{r}'_2)^2} G_{\mathbb{P}}(0, \xi_{\mathbf{r}'_1 + \mathbf{r}'_2, R}) \\
& - \frac{1}{2} \int G_{\mathbb{P}}(0, \xi_{r_1, r'_1}) G_{\mathbb{P}}(0, \xi_{r_2, r'_2}) d^2 r'_1 K(\mathbf{r}'_1, \mathbf{r}'_2 | \mathbf{r}'_1 + \mathbf{r}'_2) \frac{d^2(\mathbf{r}'_1 + \mathbf{r}'_2)}{(\mathbf{r}'_1 + \mathbf{r}'_2)^2} G_{\mathbb{P}}(Y, \xi_{\mathbf{r}'_1 + \mathbf{r}'_2, R})
\end{aligned} \tag{31}$$

Using the initial conditions of Eq. (5b) one obtain:

$$\begin{aligned}
\bar{\rho}_2(Y; \mathbf{r}_1, \mathbf{b}_1, \mathbf{r}_2, \mathbf{b}_2) &= \frac{1}{2} \int_0^{\xi_1} d\xi' G_{\mathbb{P}}(Y, \xi_1 - \xi') G_{\mathbb{P}}(Y, \xi_2 - \xi(R)) - \frac{1}{2} \int^{\xi(\mathbf{r}'_1 + \mathbf{r}'_2)} d\xi' G_{\mathbb{P}}(Y, \xi') \\
&= G_{\mathbb{P}}(Y, \xi_1 - \xi(R)) G_{\mathbb{P}}(Y, \xi_2 - \xi(R)) - G_{\mathbb{P}}(Y, \xi_{\mathbf{r}_1 + \mathbf{r}_2, R})
\end{aligned} \tag{32}$$

The contribution of ρ_2 to the t-channel unitarity from Eq. (2) has the form:

$$\begin{aligned}
A_2(Y, r, R; \mathbf{b}) &= -2 \int d^2 r_1 d^2 r'_2 d^2 b'_1, d^2 b'_2 d^2 \delta b_1, d^2 \delta b_2 \\
&\gamma^{BA}(r_1, r'_1, \mathbf{b}_1 - \mathbf{b}'_1 \equiv \delta \mathbf{b}_1) \gamma^{BA}(r_2, r'_2, \mathbf{b}_2 - \mathbf{b}'_2 \equiv \delta \mathbf{b}_2) \rho_2(Y - Y_0, \mathbf{r}_1, \mathbf{r}_2, \mathbf{b}_1, \mathbf{b}_2) \rho_2(Y - Y_0, \mathbf{r}'_1, \mathbf{r}'_2, \mathbf{b}'_1, \mathbf{b}'_2)
\end{aligned}$$

Plugging Eq. (32) into Eq. (33) and integrating over all r 's and b 's we obtain the contribution which graphic form is shown in Fig. 6

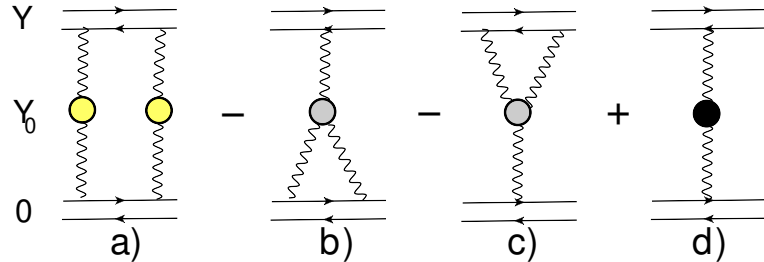


FIG. 6: The graphic form of the contributions of ρ_2 to the scattering amplitude (see Eq. (33)). The wavy lines denote the BFKL Pomeron exchanges. The gray circles denote the triple Pomeron vertex, given by the BFKL kernel. The yellow circles corresponds to integration over γ^{BA} in Eq. (33). The black circle stands for the contribution to the intercept of the BFKL Pomeron of the order of $\bar{\alpha}_S^2$.

Using the t-channel unitarity for the BFKL Pomeron [11, 30, 33] we have

$$G_{\mathbb{P}}(z) = \int \frac{d^2 r_1 d^2 r'_1 d^2 b_1 d^2 b'_1}{r_1^4 r_2^4} G_{\mathbb{P}}(Y - Y_0, \xi_{r, r_1}) \gamma^{BA}(r_1, r'_1, \mathbf{b}_1 - \mathbf{b}'_1 \equiv \delta \mathbf{b}_1) G_{\mathbb{P}}(Y_0, \xi_{r'_1, R}) \tag{33}$$

where is determined by Eq. (9) : $z = 4\bar{\alpha}_S Y + \xi_{r, R}$. Bearing this in mind we see that the diagram Fig. 6-a is equal to the exchange of two Pomeons and does not depend on Y_0 being proportional to $G_{\mathbb{P}}^2(Y - Y_0, \xi_{r, r_1}) G_{\mathbb{P}}^2(Y_0, \xi_{r'_1, R}) = G_{\mathbb{P}}^2(Y, \xi_{r, R}) = \exp(4\bar{\alpha}_S Y)$. The diagrams Fig. 6-b and Fig. 6-c do depend on Y_0 and they are suppressed by a factor $\exp(-2\bar{\alpha}_S(Y - Y_0)) (\exp(-2\bar{\alpha}_S Y_0))$ in comparison with Fig. 6-a, respectively. These diagrams belong to the BFKL Pomeron calculus but have to be integrated over Y_0 . At fixed Y_0 they have to be viewed as corrections. Fig. 6-d gives a contribution to the intercept of the Pomeron of the order of $\bar{\alpha}_S^2$. However, since its position is fixed at $Y = Y_0$ this diagram cannot describe the contribution of the next order corrections to the Pomeron intercept in the scattering amplitude. Hence, all diagrams except Fig. 6-a lead to the correction in summing of the large Pomeron loops. In other words, for summing the contributions of the large Pomeron loops to the scattering amplitude we need to account only for the contributions to ρ_n of the following form:

$$\rho_n(Y - Y_0, \{\mathbf{r}_i, \mathbf{b}_i\}) = C_n \prod_{i=1}^n G_{\mathbb{P}}(z_i) \quad \text{with} \quad z_i = 4\bar{\alpha}_S(Y - Y_0) + \xi_{r_i, r} \tag{34}$$

where r is the size of the incoming dipole. C_n is a constant which value could depend on r .

IV. BK SCATTERING AMPLITUDE IN THE BFKL POMERON CALCULUS

Using Eq. (2) and Eq. (34) we can calculate dipole-nucleus amplitude putting $Y_0 = 0$ (see Fig. 2). For ρ_n of the nucleus we consider a nucleus as a bag of dipoles with size R which do not interact with each other at $Y_0 = 0$. It means that (see Eq. (5b) and Fig. 2)

$$\rho_n^A(Y_0 = 0, r', b', \{\mathbf{r}'_i, \mathbf{b}'_i\}) = \frac{S_A^n(b')}{n!} \prod_{i=1}^n \delta^{(2)}(\mathbf{r}'_i - \mathbf{R}) \delta^{(2)}(\mathbf{b}' - \mathbf{b}_i); \quad (35)$$

Factor $S_A^n(b')$ describes the probability to find n - nucleons (dipoles) in a nucleus at the impact parameter b' .

Plugging Eq. (35) into Eq. (2) we obtain:

$$A_A^{dip}(Y, r, R; \mathbf{b}) = \sum_{n=1}^{\infty} C_n (-1)^n \prod_{i=1}^n \int \frac{d^2 r_i}{r_i^2} G_{IP}(Y, \xi_r) \gamma_A^{BA}(r_i, b) G_{IP}(Y_0, \xi_{r'_i, R}) \quad (36)$$

where $\gamma_A^{BA}(r_i, b)$ is the amplitude of scattering of the dipole with size r_i with the nucleus at small energies. Using Eq. (33) we can rewrite this equation in the following form:

$$N_A^{dip}(Y, r, R; \mathbf{b}) = \sum_{n=1}^{\infty} C_n (-1)^{n-1} G_{IP}^n(Y, \xi_{r, R}, b) \quad (37)$$

where $G_{IP}(Y, \xi_{r, R}, b) = N_0 \exp(\frac{1}{2}z_A)$ with $z_A = 4\bar{\alpha}_S Y + \xi_{r, R_A} = 4\bar{\alpha}_S Y + \ln(r^2 Q_A(Y=0, b))$. $Q_A(Y=0, b) = Q_0 S_A(b)$.

Eq. (37) shows that we can find coefficients C_n in Eq. (34) by finding the BK amplitude $N_A^{dip}(Y, r, R; \mathbf{b})$ as a series of many BFKL Pomeron exchange. In other words, we can find C_n from Eq. (18) by rewriting it as the equations for C_n . Plugging Eq. (37) into Eq. (18) we have the following equations for C_n :

$$2nC_n = \frac{2}{n}C_n - 2 \sum_{k=1}^n \frac{C_k C_{n-k}}{k} = \frac{2}{n}C_n + n \sum_{k=1}^n \frac{C_k C_{n-k}}{k(n-k)} \quad (38)$$

Denoting C_n/n by c_n we obtain:

$$2(n^2 - 1)c_n = n \sum_{k=1}^n c_k c_{n-k} \quad (39)$$

The recurrent relation has the initial condition $C_1 = 1$, which give $c_2 = 1/3, c_3 = 1/8$. At large n Eq. (39) has solution: $c_n = 2e^{\alpha} n$ with arbitrary α . However, this solution does not reproduces the large z asymptotic behaviour of Eq. (1)[63]. We first rewrite Eq. (37) as the integral over n . It takes the form (see Fig. 7):

$$N_A^{dip}(Y, r, R; \mathbf{b}) = \oint_C \frac{dn}{2\pi i} C_n \frac{\pi}{\sin(\pi n)} G_{IP}^n(Y, \xi_{r, R}, b) \quad (40)$$

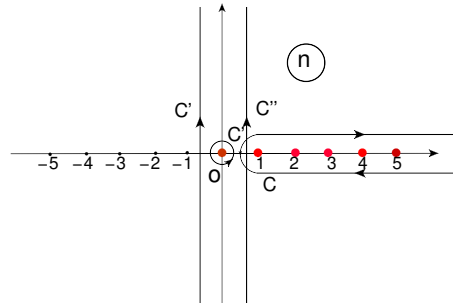


FIG. 7: The contours of integration in Eq. (40). The red points denote the poles in n .

Bearing in mind Eq. (40) we can view n and k as continuous variable, replacing Eq. (39) as follows:

$$2(n^2 - 1)c_n = n \int_1^{n-1} dk c_k c_{n-k} \quad (41)$$

We are looking for the solution in the form: $c_n = \phi(n) \exp(\frac{1}{2}n^2)$ where $\phi(n)$ is a smooth function of n in comparison with $\exp(\frac{1}{2}n^2)$. With such c_n the integral over k in Eq. (41) can be taken using the method of steepest decent, since the integrant has to strong maxima at the limits of integrations: $k = 1$ and $k = n - 1$. Introducing a new variable $k = 1 + \delta k$ in the first maximum, one can see that the main contribution comes from small $\delta k \sim 1/n$ at large n . Rewriting $\frac{1}{2}((n-k)^2 + k^2)$ as $\frac{1}{2}(n-1)^2 - n\delta k + 2\delta k^2$ one can see that the equation takes the form at large n :

$$2n^2 \phi(n) = 2\phi(n+1/n) \phi(1+1/n) e^{-n+2/n} \quad (42)$$

with the solution

$$\phi\left(1 + \frac{1}{n}\right) = n^2 e^n; \quad \phi(x) = \frac{1}{(1-x)^2} \exp\left(\frac{1}{x-1}\right) \quad (43)$$

Finally for large n we have

$$C_n = \frac{1}{n} \exp\left(\frac{1}{2}n^2 - 2n\right) \quad (44)$$

Plugging this solution to the scattering amplitude of Eq. (40) we obtain:

$$N_A^{dip}(Y, r, R; \mathbf{b}) = \oint_C \frac{dn}{2\pi i n} \frac{1}{n} \exp\left(\frac{1}{2}n^2 - 2n\right) \frac{\pi}{\sin(\pi n)} G_P^n(Y, \xi_{r,R}, b) = \oint_C \frac{dn}{2\pi i n} \frac{1}{n} \exp\left(\frac{1}{2}n^2 - 2n\right) \frac{\pi}{\sin(\pi n)} e^{\frac{1}{2}n z_A} \quad (45)$$

This equation is a good illustration of a general fact that the multi-Pomeron expansion appears as a badly divergent series. Summation of asymptotic series implies finding an analytical function with identical series expansion. In general, this asymptotic series cannot be summed even via Borel resummation[64]. Fortunately, Ref.[10] has solved the main difficult problems that we are faced with the resummation of the asymptotic series of Eq. (45) type. The first problem is that $C_n \propto \exp(\frac{1}{2}n^2)$ which makes Eq. (45) not Borel summable. Plugging in Eq. (45) the integral representation for $C_n = \exp(\frac{1}{2}n^2)$:

$$\exp\left(\frac{1}{2}n^2\right) = \frac{1}{\sqrt{2\pi}} \int_{-\infty}^{\infty} d\lambda \exp\left(-\frac{1}{2}\lambda^2 - n\lambda\right) \quad (46)$$

one can see that the asymptotic series at fixed λ can be summed *a la* Borel[64] and can be extended by analytic continuation to any value of n in the right half-plane. Therefore, we can integrate Eq. (45) along the contour C' in Fig. 7. Using the Borel prescription we rewrite this equation in the following form:

$$N_A^{dip}(Y, r, R; \mathbf{b}) = \oint_{C'} \frac{dn}{2\pi i} \int_0^{\infty} dt e^{-t} \frac{1}{n} \exp\left(\frac{1}{2}n^2 - 2n\right) \frac{\pi}{\sin(\pi n)} \frac{t^n}{\Gamma(n+1)} e^{\frac{1}{2}n z_A} \quad (47a)$$

$$= \oint_{C'} \frac{dn}{2\pi i} \int_0^{\infty} dt e^{-t} \frac{1}{n} \exp\left(\frac{1}{2}n^2 - 2n\right) \Gamma(-n) t^n e^{\frac{1}{2}n z_A} \quad (47b)$$

$$= 1 + \int_{-\epsilon-i\infty}^{-\epsilon+i\infty} \frac{dn}{2\pi i} \int_0^{\infty} dt e^{-t} \frac{1}{n} \exp\left(\frac{1}{2}n^2 - 2n\right) \Gamma(-n) t^n e^{\frac{1}{2}n z_A} \quad (47c)$$

In Eq. (47a) and Eq. (47b) the formulae **8.332(2)**, **8.334** of Ref.[69] are used. In Eq. (47c) we integrated over the pole at $n = 0$. Note that we assumed that $C_{n=0}$ is equal to 1. It goes without saying that Eq. (44) cannot provide us with the analytic continuation of C_n at small values of n .

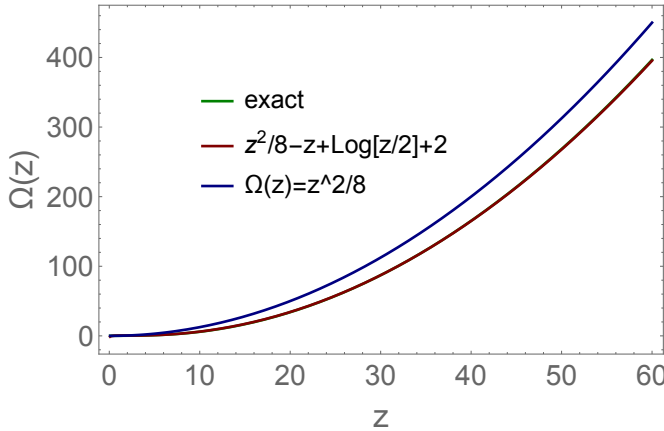


Fig. 8-a

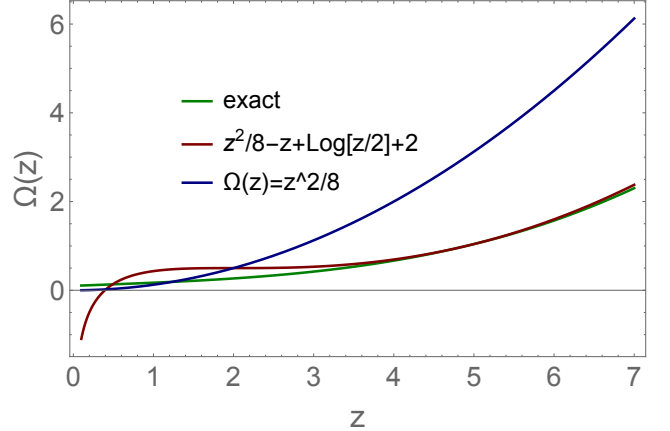


Fig. 8-b

FIG. 8: $\Omega(z)$ versus z . Ω_{exact} is the numerical solution of Eq. (23) with $\Omega_0 = 0.1$. $\Omega(z) = \frac{1}{8}z_A^2 - z_A + \ln\left(\frac{1}{2}z_A\right)$ is our approximation for Ω that is coming from the large n behaviour of the coefficient C_n in the Pomeron expansion of Eq. (50). $\Omega = z^2/8$ is the asymptotic solution of Ref.[8].

Taking the integral in Eq. (47c) using the steepest decent method we see that $n_{SP} = -\frac{1}{2}z_A$ and the scattering amplitude is equal to

$$N_A^{dip}(Y, r, R; \mathbf{b}) = 1 - \exp\left(-\frac{1}{8}z_A^2 + z_A - \ln\left(\frac{1}{2}z_A\right) - 2\right) \quad (48)$$

Therefore, we reproduce Eq. (1) and fixed the value of the smooth function $C(z)$. For the phase $\Omega(z_A)$ we have

$$\Omega(z_A) = \frac{1}{8}z_A^2 - z_A + \ln\left(\frac{1}{2}z_A\right) + 2 \quad (49)$$

In Fig. 8 we compare this solution with the exact numerical solution of Eq. (39). One can see that we found a good approximation for $z \geq 4$. Our main problem that we found the solution to the master equation (see Eq. (38) only in the region of large n . Hence, we cannot use the initial condition $C_1 = 1$ to determine all coefficients. In particularly the general form of solution:

$$C_n = \frac{1}{n} \exp\left(\beta \frac{1}{2}n^2 - 2\alpha n\right) \quad (50)$$

with arbitrary coefficients β and α is also the solution. Therefore, $\alpha = \beta = 1$ is our preferable choice. Since, these values lead to good descriptions at small values of z_A (see Fig. 8-b) we can hope that our C_n could describe the region of small n . It is instructive to note that $-z_A + 2$ term in Eq. (49) comes from the choice $\alpha = 1$ while $\ln(z_A/2)$ term reflects $1/n$ behaviour of C_n .

V. MULTIPLICITY DISTRIBUTION AND ENTROPY OF PRODUCED GLUONS FOR BK SCATTERING AMPLITUDE

In this section we are going to make use of the advantage of the multi Pomeron expansion for the scattering amplitude (see series of Eq. (37) to obtain the multiplicity distribution of produced gluons for BK scattering amplitude. Our approach consists of two steps (see Ref.[2, 11]). First, we recall that it is proven in Refs.[5] that the s -channel unitarity for the BFKL Pomeron has the form:

$$2 \operatorname{Im} G_{IP}(z) = \sigma_{in}^{\text{BFKL}}(z) \quad (51)$$

where $G_{\mathcal{P}}$ is the Green's function for the BFKL Pomeron. $\sigma_{in}^{\text{BFKL}}(z)$ is the inelastic cross sections of produced gluons, which have the Poisson distribution with this mean multiplicity $\bar{n} = \frac{1}{2}z$ (see Appendix A of Ref.[2]).

The second step is the AGK cutting rules[66], which allow us to calculate the imaginary part of the scattering amplitude, that determines the cross sections, through the powers of $\text{Im } G^{\text{BFKL}}(z)$ ⁵. Our master formula takes the form of convolution for the cross section of produced n gluons:

$$\sigma_n(z) = \sum_k \underbrace{\sigma_k^{\text{AGK}}(z)}_{\propto (\text{Im } G_{\mathcal{P}})^k} \underbrace{\frac{(k \frac{1}{2} z)^n}{n!} e^{-k \frac{1}{2} z}}_{\text{Poisson distribution}} \quad (52)$$

The AGK cutting rules [66] allows us to calculate the contributions of n -cut Pomerons if we know F_k : the contribution of the exchange of k -Pomerons to the cross section. They take the form:

$$n \geq 1 : \sigma_n^k(Y, \xi_{r,R}) = (-1)^{n-k} \frac{k!}{(n-k)! n!} 2^k F_k(Y, \xi_{r,R}) \quad (53a)$$

$$n = 0 : \sigma_0^k(Y) = (-1)^k \left(2^k - 2 \right) F_k(Y, \xi_{r,R}); \quad (53b)$$

$$\sigma_{tot} = 2 \sum_{k=1}^{\infty} (-1)^{k+1} F_k(Y, \xi_{r,R}); \quad (53c)$$

$\sigma_{tot} = 2 \text{Im } A(z)$ where A is the scattering amplitude. σ_0 is the cross section of diffractive production of small numbers of gluons which is much smaller than ΔY . First we rewrite Eq. (37) in more convenient form to find $F_k(Y, \xi_{r,R})$:

$$N_A^{dip}(Y, r, R; \mathbf{b}) = \int_{-\infty}^{\infty} d\lambda e^{-\frac{1}{2}\lambda^2} \sum_{n=1}^{\infty} (-1)^{n-1} e^{\frac{1}{2}n(z_A - 4 - 2\lambda)} = \int_0^{\infty} dt \int_{-\infty}^{\infty} d\lambda e^{-\frac{1}{2}\lambda^2} \sum_{n=1}^{\infty} (-1)^{n-1} e^{\frac{1}{2}n(z_A - 4 - 2\lambda - 2t)} \quad (54)$$

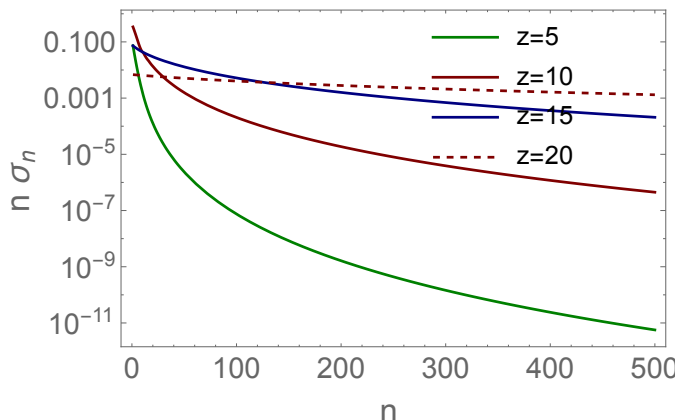


Fig. 9-a

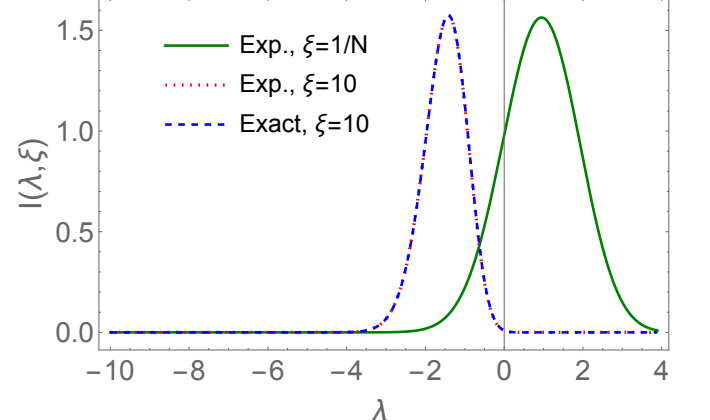


Fig. 9-b

FIG. 9: Fig. 9-a: Multiplicity distributions for BK scattering process of Eq. (55d). Fig. 9-b: Integrant of the first term in Eq. (55d) as a function of λ at fixed $\xi = \frac{n+1}{N(z_A)}$. For $\xi = 10$ the integrant is multiplied by factor 200. For $\xi = 1/N$ N is taken to be equal to $N(z_A = 15)$.

⁵ In the widespread slang this contribution is called by cut Pomeron.

Plugging $F_k(Y, \xi_{r,R})$ from Eq. (54) into Eq. (53a) and using a new notation: $N(z) = N_0 \exp(\frac{1}{2}(z-4))$ we obtain:

$$\sigma_n(z) = \sum_{k=n}^{\infty} \sigma_n^k(z) = \int_0^{\infty} dt \int_{-\infty}^{\infty} d\lambda e^{-\frac{1}{2}\lambda^2} \sum_{k=n}^{\infty} (-1)^{k-n} \frac{k!}{(k-n)! n!} \left(\frac{1}{2}N(z_A)\right)^k e^{-k\lambda - k t} \quad (55a)$$

$$= \int_0^{\infty} dt \int_{-\infty}^{\infty} d\lambda e^{-\frac{1}{2}\lambda^2} \frac{N^n(z_A) e^{-n\lambda - n t}}{(1 + N(z_A) e^{-\lambda - t})^{n+1}} \quad (55b)$$

$$= \frac{1}{n} \int_{-\infty}^{\infty} d\lambda e^{-\frac{1}{2}\lambda^2} \frac{N^n(z_A) e^{-n\lambda}}{(1 + N(z_A) e^{-\lambda})^{n+1}} \quad (55c)$$

$$= \frac{1}{n N(z_A)} \int_{-\infty}^{\ln N(z_A)} d\lambda e^{-\frac{1}{2}\lambda^2} \frac{e^{\lambda}}{\left(1 + \frac{e^{\lambda}}{N(z_A)}\right)^{n+1}} + \frac{1}{n} \int_{\ln N(z_A)}^{\infty} d\lambda e^{-\frac{1}{2}\lambda^2} \frac{N^n(z_A) e^{-n\lambda}}{(1 + N(z_A) e^{-\lambda})^{n+1}} \quad (55d)$$

$$\xrightarrow{n \gg 1, z \gg 1} \frac{\sqrt{2e\pi}}{2n} e^{-\frac{1}{2}(z-4)} + \frac{1}{n(\frac{1}{2}(z-4+2\ln 2+n))} e^{-\frac{(z-4)^2}{8}} \quad (55e)$$

The multiplicity distribution of Eq. (55d) is shown in Fig. 9. One can see that σ_n falls down at large n . This decrease is faster than $1/n$. Eq. (55e) we obtain neglecting $\frac{e^{\lambda}}{N(z_A)}$ in the first term and $N(z_A) e^{-\lambda}$ in the second one. The main contribution comes from the first term, which actually we can interpret as the multiplicity distribution of the first term (1) of the scattering amplitude in Eq. (48). It should be mentioned that factor $1/n$ is not valid in this region as we have discussed in the previous section. Therefore, we believe that we have to take off this factor and discuss Fig. 9 as given for σ_n . It should be emphasized that the first term of Eq. (55e) (with the factor $1/n$) leads to $\sigma_{in} = \sum_{n=1}^{\infty} \sigma_n \propto \frac{1}{2}(z_A - 4)$ in the violation of the s-channel unitarity.

We are going to discuss the first term of Eq. (55d) rewriting it in more convenient form:

$$\underbrace{\frac{1}{N(z_A)} \int_{-\infty}^{\ln N(z_A)} d\lambda \frac{e^{-\frac{1}{2}\lambda^2 + \lambda}}{\left(1 + \frac{e^{\lambda}}{N(z_A)}\right)^{n+1}}}_{\text{Exact}} = \underbrace{\frac{1}{N(z_A)} \int_{-\infty}^{\ln N(z_A)} d\lambda e^{-\frac{1}{2}\lambda^2 + \lambda} \exp\left(-(n+1)\frac{e^{\lambda}}{N(z_A)}\right)}_{\text{Exp.}} = \underbrace{\frac{1}{N(z_A)} \int_{-\infty}^{\ln N(z_A)} d\lambda e^{-\frac{1}{2}\lambda^2 + \lambda - \xi e^{\lambda}}}_{\text{Exp.}} \quad (56)$$

In Fig. 9-b we plot the integrants ($I(\lambda, \xi)$) of Eq. (56). One can see that (i) $I(\lambda, \xi)$ have clear maximum, (ii) the position of the maximum is away of the upper limit of integration ($\ln N(z_A)$) and (iii) the approximate expression (Exp. in Eq. (56)) works quite well. Based on these features we can state that σ_n display the KNO scaling behaviour [71], viz:

$$\sigma_n = \frac{1}{N(z_A)} \Psi\left(\frac{n}{N(z_A)}\right) \quad (57)$$

We use the steepest decent method to calculate Ψ function with the following equation for the saddle point in λ :

$$1 - \lambda_{SP} - \xi e^{\lambda_{SP}} = 0; \quad (1 - \lambda_{SP}) e^{1 - \lambda_{SP}} = e \xi; \quad (58)$$

The second equation is the Lambert equation for $1 - \lambda_{SP}$ leading to

$$1 - \lambda_{SP} = W(e \xi) \quad (59)$$

For Lambert function we have the series representation:

$$1 - \lambda_{SP} = W(e \xi) = \sum_{n=1}^{\infty} \frac{(-n)^{n-1}}{n!} (e \xi)^n \quad (60)$$

and the asymptotic behaviour:

$$W(e \xi) = \ln\left(\frac{e \xi}{\ln(e \xi)}\right); \quad \lambda_{SP} = -\ln \xi + \ln(1 + \ln \xi) \quad (61)$$

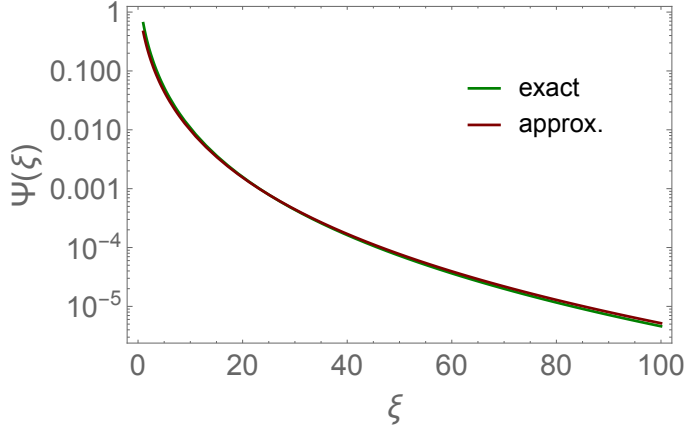


FIG. 10: The KNO function Ψ versus $\xi \equiv \frac{n}{N(z_A)}$. Exact is the numerical calculation of Eq. (56) while Approx. stands for the solution of Eq. (62).

Using this equation for λ_{SP} we obtain:

$$\Psi\left(\xi \equiv \frac{n}{N(z_A)}\right) = \sqrt{\frac{\pi}{2}} \exp\left(-\frac{1}{2}\lambda_{SP}^2 + \lambda_{SP} - \xi e^{\lambda_{SP}}\right) \quad (62)$$

Fig. 10 shows the KNO function from the exact calculation of the integral in Eq. (56) and from Eq. (62). For large ξ we have $\lambda_{SP} = -\xi$ and

$$\Psi\left(\xi \equiv \frac{n}{N(z_A)}\right) \propto e^{-\frac{1}{2}\xi^2} \quad (63)$$

VI. DIPOLE-DIPOLE SCATTERING AMPLITUDE

Using Eq. (50) we obtain the dipole densities for fast moving dipole with the size r and rapidity Y ρ_n in the form:

$$\rho_n(Y\{\mathbf{r}_i, \mathbf{b}_i\}) = \frac{1}{n} \exp\left(\beta \frac{1}{2} n^2 - 2\alpha n\right) \prod_{i=1}^n G_{IP}(z_i) \quad \text{with} \quad z_i = 4\bar{\alpha}_S Y + \xi_{r_i, r} \quad (64)$$

From Eq. (2) we can calculate the dipole-dipole amplitude (N) summing the large Pomeron loops. We have for the S-matrix of scattering the dipole with size r and rapidity Y

$$S(z) = 1 - N(z) = \sum_{n=0}^{\infty} (-1)^n n! C_n^2 \int d^2 r_i d^2 r'_i d^2 b_i d^2 b'_i \prod_{i=1}^n \frac{G_{IP}(z_i)}{N_0} \gamma^{BA}(r_i, r'_i, \delta b) \frac{G_{IP}(z'_i)}{N_0} \quad (65)$$

Applying the t-channel unitarity to the BFKL Pomeron exchange (see Eq. (33)) we reduce Eq. (66) to the following equation:

$$S(z) = 1 - N(z) = \sum_{n=0}^{\infty} (-1)^n n! C_n^2 \left(\frac{G_{IP}(z')}{N_0^2}\right)^n \quad (66)$$

Repeating all steps that we have been discussed in Eq. (40) and Eq. (46) -Eq. (47b), we turn Eq. (66) into:

$$S(z) = 1 - N(z) = \oint_{C'} \frac{dn}{2\pi i} \int_0^{\infty} dt e^{-t} n! \frac{1}{n^2} e^{n^2 - 4n} \left(\frac{e^{\frac{1}{2}z'}}{N_0^2}\right)^n t^n \quad (67)$$

Note, that contour C' in this equation does not include the pole at $n = 0$ since we consider the S-matrix.

Taking this integral by the method of steepest descent with the saddle point $n_{SP} = -\frac{1}{4}z'$, we obtain:

$$S(z) = \frac{8}{\sqrt{\pi}} \frac{1}{z'^2} \exp \left(-\frac{z'^2}{16} + z' - \frac{1}{4}z'(\ln(z'/4) - 1) \right) \quad (68)$$

From this equation one can see that we reproduce the results for the dipole-dipole scattering amplitude both from the estimates of the rare fluctuation in the CGC [24, 25] and from the BFKL Pomeron calculus in our previous works[2–4]. The scattering amplitude that we obtained, turns out to be very close to our approach, based on Eq. (1) (see Refs. [2–4]), but it is more economic and straightforward. We wish to use the great advantage of the multi-Pomeron expansion of the scattering amplitude, considering multiplicity distributions of the produced gluons for dipole-dipole scattering processes.

VII. MULTIPLICITY DISTRIBUTION OF PRODUCED GLUONS FOR DIPOLE-DIPOLE SCATTERING

Using Eq. (66) for the dipole-dipole scattering amplitude with C_n from Eq. (44) and rewriting e^{n^2} as follows:

$$e^{n^2} = 2\sqrt{\pi} \int_{-\infty}^{\infty} d\lambda e^{-\frac{\lambda^2}{4} + n\lambda} \quad (69)$$

we obtain the amplitude in the form:

$$N(z') = \frac{1}{2\sqrt{\pi}} \sum_{n=1}^{\infty} \frac{(-1)^{n+1}}{n^2} \int_{-\infty}^{\infty} d\lambda e^{-\frac{\lambda^2}{4} + n\lambda} n! G^n(z') = \frac{1}{2\sqrt{\pi}} \sum_{n=1}^{\infty} \frac{(-1)^n}{n^2} \int_{-\infty}^{\infty} d\lambda e^{-\frac{\lambda^2}{4} + n\lambda} \int_0^{\infty} dt e^{-t} t^n G^n(z') \quad (70)$$

In this equation we introduce the integral representation for $\Gamma(n+1)$. As we have discussed in the previous section factor $1/n^2$ cannot to be valid at small values of n which contribute to the asymptotic value of $N(z') = 1$. Indeed, taking this factor off we can sum over n and take the integral with respect to t . The answer is

$$N(z') = \frac{1}{2\sqrt{\pi}} \int_{-\infty}^{\infty} d\lambda e^{-\frac{\lambda^2}{4}} \left(1 - \frac{e^{1/(e^{\lambda} G(z'))} \Gamma(0, \frac{1}{(e^{\lambda} G(z'))})}{e^{\lambda} G(z')} \right) \quad (71)$$

The first term gives 1 while the second leads to the contribution of Eq. (68). Therefore, to reconstruct the multiplicity distribution at large z' we need to take off the factor $1/n^2$. However, we have to put it back if we wish to discuss corrections proportional to $\exp(-\frac{z'^2}{16})$.

Applying the AGK cutting rules of Eq. (53a), Eq. (53b) to this amplitude one can see that σ_n is equal to

$$\begin{aligned} \sigma_n(z') &= \frac{1}{2\sqrt{\pi}} \sum_{k=n}^{\infty} (-1)^{k-n} \left(\frac{k!}{(k-n)! n!} \right) \int_{-\infty}^{\infty} d\lambda e^{-\frac{\lambda^2}{4}} \int_0^{\infty} dt (t e^{-t+\lambda} G(z'))^n \\ &= \frac{1}{2\sqrt{\pi}} \int_{-\infty}^{\infty} d\lambda e^{-\frac{\lambda^2}{4}} \int_0^{\infty} dt e^{-t} \frac{(t e^{\lambda} N(z'))^n}{(1 + t e^{\lambda} N(z'))^{n+1}} = \frac{n!}{2\sqrt{\pi}} \int_{-\infty}^{\infty} d\lambda e^{-\frac{\lambda^2}{4}} \frac{1}{e^{\lambda} N(z')} U\left(n+1, 1, \frac{1}{e^{\lambda} N(z')}\right) \end{aligned} \quad (72)$$

where $U\left(n+1, 1, \frac{1}{e^{\lambda} N(z')}\right)$ is the Tricomi confluent hypergeometric function (see Ref.[72], formula 13.1.3). This function has two interesting limits:

$$\frac{n!}{e^\lambda N(z')} U\left(n+1, 1, \frac{1}{e^\lambda N(z')}\right) \rightarrow \begin{cases} \frac{1}{e^\lambda N(z')} K_0\left(2\sqrt{\frac{n+1}{e^\lambda N(z')}}\right) & \text{for } e^\lambda N(z') > 1; \\ \frac{n!}{e^\lambda N(z')}\left(n + \frac{1}{e^\lambda N(z')}\right)^{-(n+1)} & \text{for } e^\lambda N(z') < 1; \end{cases} \quad (73)$$

For these two regions Eq. (72) can be rewritten as follows:

$$\sigma_n(z') = \frac{1}{2\sqrt{\pi}} \int_{-\ln N(z')}^{\infty} d\lambda e^{-\frac{\lambda^2}{4}} \frac{1}{e^\lambda N(z')} K_0\left(2\sqrt{\frac{n+1}{e^\lambda N(z')}}\right) + \frac{1}{2\sqrt{\pi}} \int_{-\infty}^{-\ln N(z')} d\lambda e^{-\frac{\lambda^2}{4}} \frac{n!}{e^\lambda N(z')} \left(n + \frac{1}{e^\lambda N(z')}\right)^{-(n+1)} \quad (74)$$

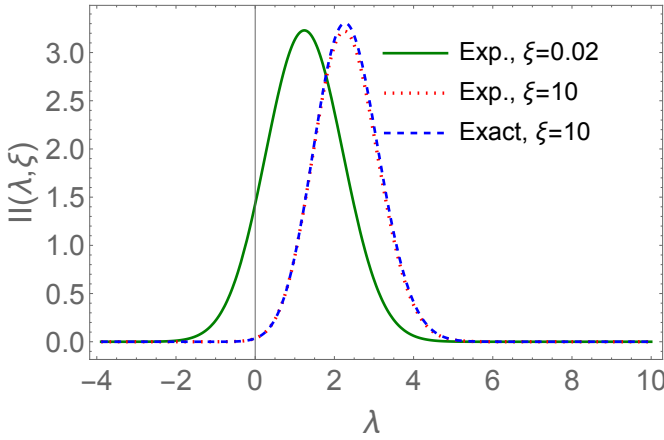


Fig. 11-a

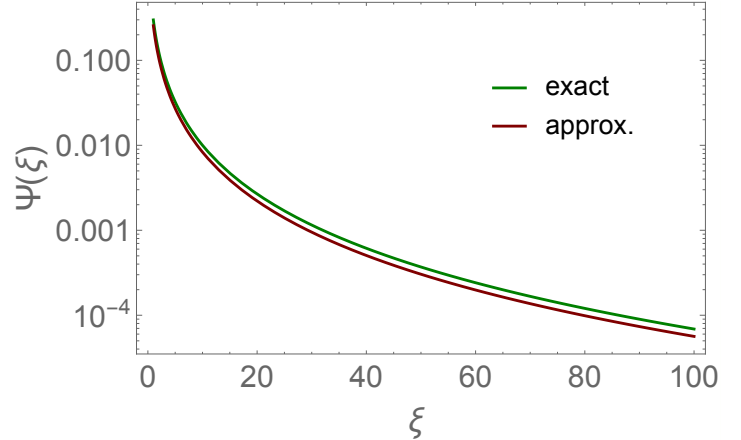


Fig. 11-b

FIG. 11: Multiplicity distributions for dipole-dipole scattering process of Eq. (75). Fig. 11-a: Integrand $II(\lambda, \xi = \frac{n+1}{N(z')})$ of the first term in Eq. (75) as a function of λ at fixed $\xi = \frac{n+1}{N(z')}$. For $\xi = 10$ the integrant is multiplied by factor 50. Fig. 11-b: The KNO function Ψ versus $\xi = \frac{n}{N(z')}$. Exact is the numerical calculation of Eq. (75) while approx. stands for the solution of Eq. (78)

The second term in Eq. (74) gives a small contribution proportional to $\exp\left(-\frac{z'^2}{16}\right)$. We rewrite the first term in the more convenient form:

$$\begin{aligned} \int_{-\ln N(z')}^{\infty} d\lambda II\left(\lambda, \xi = \frac{n+1}{N(z')}\right) &= \frac{1}{2\sqrt{\pi}} \int_{-\ln N(z')}^{\infty} d\lambda e^{-\frac{\lambda^2}{4}} \underbrace{\frac{1}{e^\lambda N(z')} K_0\left(2\sqrt{\frac{\xi}{e^\lambda}}\right)}_{\text{exact}} \\ &= \frac{1}{2\sqrt{2}} \int_{-\ln N(z')}^{\infty} d\lambda e^{-\frac{\lambda^2}{4}} \underbrace{\frac{1}{e^\lambda N(z')} \sqrt{2\sqrt{\frac{\xi}{e^\lambda}}}}_{\text{approx.}} \exp\left(-2\sqrt{\frac{\xi}{e^\lambda}}\right) \end{aligned} \quad (75)$$

Fig. 11 shows the λ dependence of $II(\lambda, \xi)$. One can see that (i) this dependence has a clear maximum; (ii) the lower limit of integration does not influence on the value of the integral; and (iii) the approximate expression for II (see approx. in Eq. (75)) describe the exact integrant quite well. Therefore, we can use the last term in Eq. (75) and take the integral using the method of steepest descent with the following equation for λ_{SP} :

$$\frac{1}{2}\lambda_{SP} + \frac{3}{4} = e^{-\frac{1}{2}\lambda_{SP}} \sqrt{\xi}; \quad \zeta_{SP} e^{\zeta_{SP}} = \frac{1}{2} e^{\frac{3}{4}} \sqrt{\xi} \quad \text{with} \quad \zeta_{SP} \equiv \frac{1}{2}\lambda_{SP} + \frac{3}{4} \quad (76)$$

The solution for ζ_{SP} is the W Lambert function which we have discussed in section V (see Eq. (58)-Eq. (61)). Therefore, the solution is

$$\zeta_{SP} \equiv \frac{1}{2}\lambda_{SP} + \frac{3}{4} = W\left(\frac{1}{2}e^{\frac{3}{4}}\sqrt{\xi}\right) : \quad \lambda_{SP} = \frac{3}{2} + 2W\left(\frac{1}{2}e^{\frac{3}{4}}\sqrt{\xi}\right) \quad (77)$$

Plugging Eq. (77) into the last equation of Eq. (75) we obtain for the KNO function Ψ : (see Eq. (57))

$$\Psi(\xi) = \sqrt{2\pi} \frac{e^{-\frac{\lambda_{SP}^2}{4} - 2\sqrt{e^{-\lambda_{SP}}\xi} + \lambda_{SP}}}{\sqrt{2}\sqrt[4]{e^{-\lambda_{SP}}\xi}} \quad (78)$$

For large ξ using Eq. (61) we obtain $\lambda_{SP} = \xi$ and

$$\Psi(\xi) \propto e^{-\frac{\xi^2}{4}} \quad (79)$$

VIII. ENTROPY OF PRODUCED GLUONS

We found that for dipole-target (BK amplitude) and dipole-dipole scattering the multiplicity distributions of produced gluons have the KNO scaling behaviour with different functions Ψ (see Eq. (62) and Eq. (78) and Fig. ??) but with the same mean multiplicity $\bar{n} = N(z')$ ⁶. This feature is enough to find the entropy at high energies which will be the same in deep inelastic scattering (DIS) and for interactions of two dipoles at high energies. Indeed for $\mathcal{P}_n = \frac{1}{\bar{n}}\Psi\left(\frac{n}{\bar{n}}\right)$ the von Neumann entropy is equal

$$\begin{aligned} S_E &= -\sum_n \ln(\mathcal{P}_n) \mathcal{P}_n = \ln \bar{n} \underbrace{\sum_n \frac{1}{\bar{n}}\Psi\left(\frac{n}{\bar{n}}\right)}_1 - \underbrace{\sum_n \ln\left(\Psi\left(\frac{n}{\bar{n}}\right)\right) \frac{1}{\bar{n}}\Psi\left(\frac{n}{\bar{n}}\right)}_{\text{Const}} \\ &= \ln \bar{n} + \text{Const} \xrightarrow{z \gg 1} \ln N(z') = \ln(G_{\mathcal{P}}(z')) \end{aligned} \quad (80)$$

Therefore, $S_E = \ln N(z_A) = \ln(G_{\mathcal{P}}(z_A))$ in accordance with the result of Ref.[70]. In Eq. (80) we used the well known fact that the gluon structure function in QCD is equal to the contribution of the exchange of one BFKL Pomeron [33]. Different form of the KNO function Ψ results in a different value of Const in Eq. (80). For Ψ of Eq. (62) this constant is equal to -1.706 while for dipole-dipole scattering its value is -0.217.

We would like to emphasize that both the value of the entropy and the multiplicity distributions at large z follows directly from QCD evolution equations and the t -channel unitarity constraints of Eq. (2). Bearing this in mind we expect to learn a lot comparing with other QCD results (see Refs.[70, 73]), which give a much larger entropy ($\propto z^2$) in QCD. We plan to clarify this discrepancy in our further publications.

It should be noted that the multiplicity distribution are quite different for DIS (BK amplitude) and for dipole-dipole scattering in spite of the same value of the entropy. Indeed, we have seen in Eq. (63) and Eq. (79) that Ψ for dipole-dipole amplitude is rather equal to $\sqrt{\Psi}$ for BK amplitude. It is instructive to note that situation turns out to be quite different from the one dimensional models in which $\Psi_{\text{dipole-dipole}}(\xi) = \Psi_{\text{BK}}(\sqrt{\xi})$ (see Refs. [11, 74]).

IX. CONCLUSIONS

In this paper we found the dipole densities (see Eq. (64)) for the leading twist BFKL kernel. These densities stem from the solution of nonlinear Balitsky-Kovchegov evolution equation for the scattering amplitude, and t -channel unitarity of Eq. (2) with the simple expression of Eq. (35) for the dipole densities of a nucleus. Recall that Eq. (35) views the nucleus as a bag of dipoles. Having these densities we use Eq. (2) to calculate the contributions of the large Pomeron loops to the scattering amplitude of dipole - dipole interactions at high energies.

It is shown in the paper that the QCD equations for dipole densities have a natural solution: the BFKL Pomeron calculus. We found the scattering amplitudes both for DIS(BK amplitude) and dipole-dipole scattering as the series of the exchanges of BFKL Pomerons and suggested how to sum the resulting asymptotic series.

⁶ For BK amplitude $z' = z_A$

All results are very close to the approach that we have developed in Refs.[2–4]. However, we wish to emphasize that our results in this paper are proven for the leading twist BFKL kernel while in Refs.[2–4] a suggestion has been made.

We have to remind that C_n of Eq. (64) have been found for large n (see Eq. (44) and Fig. 8-a). As we have shown (see Fig. 8-b) we could rely on their value for $z \geq 4$.

We wish to point out that our amplitude gives the same asymptotic behaviour at large z as was calculated in Ref.[8, 24]. This result not only confirms the general idea of Ref.[24] that 'rare' fluctuation contributes to the high energy behaviour of the scattering amplitude but it gives a possibility to calculate its value in the approach based on the BFKL Pomeron calculus.

We hope that our result will stimulate the study of the BFKL Pomeron calculus for finding larger contribution to the scattering matrix. In particular, we have to approach the enhanced diagrams which are crucially dependent on the small Pomeron loops.

We obtain our S-matrix from the BFKL Pomeron calculus which allow us to study the multiplicity distribution of the produced gluons using AGK cutting rules. We wish to draw the attention of a reader to the fact that actually we discuss in the paper the multiplicity distributions that correspond to the asymptotic contributions to the scattering amplitudes : $N = 1$.

It turns out that these secondary gluons have the KNO distribution. For both reaction we obtain the same average multiplicity of the produced gluons, which is equal to the gluon structure function deep in the saturation region. In spite of the fact that the multiplicity distributions have different forms for BK and dipole-dipole amplitude, the same average multiplicity results in the same entropy which is equal to $S_E = \ln(xG(x, Q^2))$ where xG is the gluon structure function. Therefore it confirms the result of Ref.[70]. It is instructive to note that the KNO function for dipole-dipole amplitude turns out to $\Psi_{\text{dipole-dipole}}(\xi) = \sqrt{\Psi_{BK}(\xi)}$ in remarkable difference from one dimensional models where $\Psi_{\text{dipole-dipole}}(\xi) = \Psi_{BK}(\sqrt{\xi})$ (see Refs. [11, 74]).

We hope that this paper will contribute to the further study of the Pomeron calculus in QCD.

Acknowledgements

We thank our colleagues at Tel Aviv university for discussions. Special thanks go A. Kovner and M. Lublinsky for stimulating and encouraging discussions on the subject of this paper. This research was supported by BSF grant 2022132.

* Electronic address: leving@tauex.tau.ac.il

- [1] E. Levin, Phys. Rev. D **107** (2023) no.5, 054012 [arXiv:2209.07095 [hep-ph]].
- [2] E. Levin, Phys. Rev. D **110** (2024) no.11, 116021 [arXiv:2409.00761 [hep-ph]].
- [3] E. Levin, Phys. Rev. D **111** (2025) no.9, 096004 [arXiv:2502.01712 [hep-ph]].
- [4] E. Levin, Phys. Rev. D **112** (2025) no.5, 054033 [arXiv:2506.07569 [hep-ph]].
- [5] V. S. Fadin, E. A. Kuraev and L. N. Lipatov, Phys. Lett. **B60**, 50 (1975); E. A. Kuraev, L. N. Lipatov and V. S. Fadin, Sov. Phys. JETP **45**, 199 (1977), [Zh. Eksp. Teor. Fiz. 72,377(1977)]; I. I. Balitsky and L. N. Lipatov, Sov. J. Nucl. Phys. **28**, 822 (1978), [Yad. Fiz. 28,1597(1978)].
- [6] I. Balitsky, Phys. Rev. **D60**, 014020 (1999); [arXiv:hep-ph/9812311];
- [7] Y. V. Kovchegov, Phys. Rev. **D60**, 034008 (1999). [arXiv:hep-ph/9901281].
- [8] E. Levin and K. Tuchin, Nucl. Phys. B **573**, 833 (2000) [hep-ph/9908317]; Nucl. Phys. A **691**, 779 (2001) [hep-ph/0012167]; **693**, 787 (2001) [hep-ph/0101275].
- [9] Yuri V. Kovchegov and Eugene Levin, "Quantum Chromodynamics at High Energies", Cambridge Monographs on Particle Physics, Nuclear Physics and Cosmology, Cambridge University Press, 2012.
- [10] A. Kovner, E. Levin and M. Lublinsky, JHEP **10** (2024), 127, [arXiv:2406.12691 [hep-ph]].
- [11] A. H. Mueller and G. P. Salam, Nucl. Phys. B **475**, 293 (1996), [hep-ph/9605302]; G. P. Salam, Nucl. Phys. B **461**, 512 (1996), [hep-ph/9509353].
- [12] E. Levin and M. Lublinsky, Phys. Lett. B **607** (2005) 131, [hep-ph/0411121]; Nucl. Phys. A **763** (2005) 172, [hep-ph/0501173].
- [13] L. N. Lipatov, Sov. Phys. JETP **63**, 904 (1986) [Zh. Eksp. Teor. Fiz. **90**, 1536 (1986)].
- [14] Y. V. Kovchegov, Phys. Rev. D **72** (2005), 094009, [arXiv:hep-ph/0508276 [hep-ph]].
- [15] E. Levin, Nucl. Phys. A **763** (2005), 140-171, [arXiv:hep-ph/0502243 [hep-ph]].

[16] P. Rembiesa and A. M. Stasto, Nucl. Phys. B **725** (2005) 251, [hep-ph/0503223].

[17] A. Kovner and M. Lublinsky, Nucl. Phys. A **767** 171 (2006), [hep-ph/0510047].

[18] A. I. Shoshi and B. W. Xiao, Phys. Rev. D **73** (2006) 094014, [hep-ph/0512206].

[19] M. Kozlov and E. Levin, Nucl. Phys. A **779** (2006) 142, [hep-ph/0604039].

[20] N. Armesto, S. Bondarenko, J. G. Milhano and P. Quiroga, JHEP 0805 (2008) 103, arXiv:0803.0820 [hep-ph].

[21] E. Levin and A. Prygarin, Eur. Phys. J. C **53** (2008) 385, [hep-ph/0701178].

[22] A. D. Le, A. H. Mueller and S. Munier, Phys. Rev. D **104**, 034026 (2021), [arXiv:2103.10088 [hep-ph]].

[23] E. Levin, Phys. Rev. D **104**, no.5, 056025 (2021), [arXiv:2106.06967 [hep-ph]].

[24] E. Iancu and A. Mueller, Nucl. Phys. A **730** (2004), 494-513 [arXiv:hep-ph/0309276 [hep-ph]];

[25] E. Iancu and A. Mueller Nucl. Phys. A **730** (2004), 460-493 [arXiv:hep-ph/0308315 [hep-ph]].

[26] A. H. Mueller and D. N. Triantafyllopoulos, Nucl. Phys. B **640** (2002) 331 [hep-ph/0205167]

[27] E. Iancu, K. Itakura and L. McLerran, Nucl. Phys. A **708** (2002) 327 [hep-ph/0203137].

[28] L. N. Lipatov, Phys. Rept. **286** (1997) 131, [hep-ph/9610276].

[29] L. N. Lipatov, Nucl. Phys. B **365**, 614 (1991), Nucl. Phys. B **452**, 369 (1995), [arXiv:hep-ph/9502308];
R. Kirschner, L. N. Lipatov and L. Szymanowski, Nucl. Phys. B **425**, 579 (1994), [arXiv:hep-th/9402010]. Phys. Rev. D **51**, 838 (1995), [arXiv:hep-th/9403082].

[30] L. V. Gribov, E. M. Levin and M. G. Ryskin, Phys. Rept. **100**, 1 (1983).

[31] E. M. Levin and M. G. Ryskin, Phys. Rept. **189**, 267 (1990).

[32] A. H. Mueller and J. Qiu, Nucl. Phys. **B268** (1986) 427.

[33] A. H. Mueller, Nucl. Phys. B **415** (1994) 373; Nucl. Phys. B **437** (1995) 107;
A. H. Mueller and B. Patel, Nucl. Phys. B 425, 471, 1994.

[34] G. P. Salam, Nucl. Phys. B **461**, 512 (1996); [hep-ph/9509353].

[35] H. Navelet and R. B. Peschanski, Nucl. Phys. B **507** (1997), 353-366 [arXiv:hep-ph/9703238 [hep-ph]].

[36] J. Bartels, Z. Phys. C **60** (1993), 471-488 ; J. Bartels and M. Wusthoff, Z. Phys. C **66** (1995), 157-1801; J. Bartels and C. Ewerz, JHEP **09** (1999), 026 [arXiv:hep-ph/9908454 [hep-ph]]; C. Ewerz, JHEP **0104** (2001) 031.

[37] J. Bartels, Nucl. Phys. **B175**, 365 (1980);
J. Kwiecinski and M. Praszalowicz, Phys. Lett. **B94**, 413 (1980).

[38] L. McLerran and R. Venugopalan, Phys. Rev. **D49** (1994) 2233, Phys. Rev. **D49** (1994), 3352; **D50** (1994) 2225; **D59** (1999) 09400.

[39] Y. V. Kovchegov and E. Levin, Nucl. Phys. B **577** (2000) 221, [hep-ph/9911523].

[40] M. A. Braun, Eur. Phys. J. **C16** (2000) 337, [arXiv:hep-ph/0001268];
M. A. Braun and G. P. Vacca, Eur. Phys. J. **C6** (1999) 147,[arXiv:hep-ph/9711486];
J. Bartels, M. Braun and G. P. Vacca, Eur. Phys. J. C **40**, 419 (2005), [arXiv:hep-ph/0412218].
J. Bartels, L. N. Lipatov and G. P. Vacca, Nucl. Phys. B **706**, 391 (2005).

[41] M. A. Braun, Phys. Lett. B **483**, 115 (2000), [hep-ph/0003004];Eur. Phys. J. C **33**, 113 (2004), [hep-ph/0309293];Phys. Lett. B **632**, 297 (2006).

[42] A. Kovner and M. Lublinsky, JHEP **02** (2007), 058 [arXiv:hep-ph/0512316 [hep-ph]].

[43] J. Jalilian-Marian, A. Kovner, A. Leonidov, and H. Weigert, , Nucl. Phys. **B504** (1997) 415–431, [arXiv:hep-ph/9701284].

[44] J. Jalilian-Marian, A. Kovner, A. Leonidov, and H. Weigert, , Phys.Rev. **D59** (1998) 014014, [arXiv:hep-ph/9706377 [hep-ph]].

[45] A. Kovner, J. G. Milhano, and H. Weigert, , Phys. Rev. **D62** (2000) 114005, [arXiv:hep-ph/0004014].

[46] E. Iancu, A. Leonidov, and L. D. McLerran, ,Nucl. Phys. **A692** (2001) 583–645, [arXiv:hep-ph/0011241].

[47] E. Iancu, A. Leonidov, and L. D. McLerran, Phys. Lett. **B510** (2001) 133–144,[arXiv:hep-ph/0102009].

[48] E. Ferreiro, E. Iancu, A. Leonidov, and L. McLerran, , Nucl. Phys. **A703** (2002) 489–538, [arXiv:hep-ph/0109115].

[49] H. Weigert, Nucl. Phys. A **703** (2002), 823-860 [arXiv:hep-ph/0004044 [hep-ph]].

[50] A. Kovner and J. G. Milhano, Phys. Rev. D **61** (2000), 014012 [arXiv:hep-ph/9904420 [hep-ph]].

[51] T. Altinoluk, A. Kovner, E. Levin and M. Lublinsky, JHEP **04** (2014), 075 [arXiv:1401.7431 [hep-ph]].

[52] A. Kovner and M. Lublinsky, Phys. Rev. D **71** (2005), 085004 [arXiv:hep-ph/0501198 [hep-ph]].

[53] A. Kovner and M. Lublinsky, Phys. Rev. Lett. **94**, 181603 (2005), [hep-ph/0502119].

[54] I. Balitsky, Phys. Rev. D **72**, 074027 (2005), arXiv:hep-ph/0507237.

[55] Y. Hatta, E. Iancu, L. McLerran, A. Stasto and D. N. Triantafyllopoulos, Nucl. Phys. A **764**, 423 (2006).,arXiv:hep-ph/0504182.

[56] A. Kovner, M. Lublinsky and U. Wiedemann, JHEP **06** (2007), 075 [arXiv:0705.1713 [hep-ph]]; T. Altinoluk, A. Kovner, M. Lublinsky and J. Peressutti, JHEP **0903**, 109 (2009), [arXiv:0901.2559 [hep-ph]].

[57] A. Kovner, E. Levin, M. Li and M. Lublinsky, JHEP **09** (2020), 199 [arXiv:2006.15126 [hep-ph]].

[58] A. Kovner, E. Levin, M. Li and M. Lublinsky, JHEP **10** (2020), 185 [arXiv:2007.12132 [hep-ph]].

[59] A. Kovner and M. Lublinsky Nucl. Phys. A **767**, 171-188 (2006),[arXiv:hep-ph/0510047 [hep-ph]].

[60] A. Kormilitzin, E. Levin and A. Prygarin, Nucl. Phys. A **813** (2008), 1-13 [arXiv:0807.3413 [hep-ph]]; E. Levin and A. Prygarin, Eur. Phys. J. C **53** (2008), 385-399 [arXiv:hep-ph/0701178 [hep-ph]].

[61] C. Contreras, E. Levin, R. Meneses and M. Sanhueza, Eur. Phys. J. C **80** (2020) no.11, 1029, [arXiv:2007.06214 [hep-ph]].

[62] J. Bartels, E. Levin, Nucl. Phys. **B387** (1992) 617-637; A. M. Stasto, K. J. Golec-Biernat, J. Kwiecinski, Phys. Rev. Lett. **86** (2001) 596-599, [hep-ph/0007192]; L. McLerran, M. Praszalowicz, Acta Phys. Polon. **B42** (2011) 99, [arXiv:1011.3403 [hep-ph]] **B41** (2010) 1917-1926, [arXiv:1006.4293 [hep-ph]].

[63] E. Levin, ‘Scattering amplitude in QCD: summing large Pomeron loops,’ [arXiv:2403.10364 [hep-ph]].

[64] Bruce Shawyer and Bruce Watson, “*Borel’s Method of Summability, Theory and Application*” , Clarendon Press, Oxford,1994;

Ovidiu Costin,“Asymptotocs and Borel Summability”, Chapman & HALL/CRC Monographs and Surveys in Pure and Applied Mathematics, CRC Press, Taylor & Francis Group,2009;
<http://www1.phys.vt.edu/ersharp/spec-fn/app-d.pdf>.

[65] A.D. Polyanin and V.F. Zaitsev “*Handbook of nonlinear partial differential equations*”, Chapman and Hall/CRC Press, 2004, Raca Baton, New York, London, Tokyo.

[66] V. A. Abramovsky, V. N. Gribov and O. V. Kancheli, *Yad. Fiz.* **18** (1973), 595, (*Sov.J. Nucl.Phys.* 18 (1974),308);

[67] S. Munier and R. B. Peschanski, *Phys. Rev. D* **69**, 034008 (2004) [[hep-ph/0310357](https://arxiv.org/abs/hep-ph/0310357)]; *Phys. Rev. Lett.* **91**, 232001 (2003) [[hep-ph/0309177](https://arxiv.org/abs/hep-ph/0309177)].

[68] A. H. Mueller and S. Munier, *Phys. Rev. D* **98** (2018) no.3, 034021, [[arXiv:1805.02847 \[hep-ph\]](https://arxiv.org/abs/1805.02847)].

[69] I. Gradstein and I. Ryzhik, *Table of Integrals, Series, and Products*, Fifth Edition, Academic Press, London, 1994

[70] D. E. Kharzeev and E. M. Levin, *Phys. Rev. D* **95** (2017) no.11, 114008 [[arXiv:1702.03489 \[hep-ph\]](https://arxiv.org/abs/1702.03489)].

[71] A.M. Polyakov, *Zh. Eksp. Teor. Fiz.* **59**, 542 (1970); Z. Koba, H.B. Nielsen and P. Olesen, *Nucl. Phys.* **B40**, 317 (1972); Z. Koba, in Proc. of the 1973 CERN School of Physics, p. 171, CERN Yellow Report CERN-73-12 (1973)

[72] M. Abramowitz and I. Stegun, “*Handbook of Mathematical Functions with Formulas, Graphs, and Mathematical Tables*”, United States Department of Commerce, National Bureau of Standards,1964.

[73] E. Levin, *Eur. Phys. J. C* **84** (2024) no.7, 662 [[arXiv:2306.12055 \[hep-ph\]](https://arxiv.org/abs/2306.12055)].

[74] E. Levin, *Phys. Rev. D* **111** (2025) no.1, 016019, [[arXiv:2412.02504 \[hep-ph\]](https://arxiv.org/abs/2412.02504)].